overemphasized canonical structures are a dianion and a neutral, than it is for an uncharged closed shell molecule, where the offending positive and negative structures have a strong coulombic attraction. It might also be argued that electron correlation is likely to be much more important in lowering the energy of the dianion than it is in the dissociation products, increasing the likelihood that the dianion might have a finite lifetime. We are grateful to the referees, who were of opposite opinions on this point, for encouraging us to discuss it.

Spectroscopy, Photophysics, and Photochemistry of Dimethyl-*s*-tetrazine and Phenyl-*s*-tetrazine in Crystals and Mixed Crystals at Low Temperatures

Robin M. Hochstrasser,* David S. King, and Amos B. Smith III*

Contribution from the Department of Chemistry, the Laboratory for Research on the Structure of Matter, and the Monell Chemical Senses Center, The University of Pennsylvania, Philadelphia, Pennsylvania 19174.
Received November 22, 1976

Abstract: The electronic absorption, fluorescence, and phosphorescence spectra of dimethyl-*s*-tetrazine and phenyl-*s*-tetrazine at low temperatures (4.2–1.6 K) are reported and analyzed in the neat and mixed crystal. The S_1–S_0 spectral origin is at 17 352 cm^{-1} for neat dimethyl-*s*-tetrazine, 17 659 cm^{-1} for neat phenyl-*s*-tetrazine, 17 001 cm^{-1} for dimethyl-*s*-tetrazine in *p*-xylene, and 17 167 cm^{-1} for phenyl-*s*-tetrazine in benzophenone; the neat crystal T_1–S_0 origin is at 13 079 cm^{-1} for dimethyl-*s*-tetrazine and 13 333 cm^{-1} for phenyl-*s*-tetrazine. The observed spectra were characteristic of symmetry allowed n–π^* transitions and correspond to the *s*-tetrazine $^{1,3}B_{3u}$–^1A_g ($n\pi^*$) transitions. Several progression forming modes were observed. The vibrational frequency in the ground state S_0 (and in the S_1 excited state in parentheses) for the methyl torsion designated X is 50 cm^{-1} (49 cm^{-1}) and the ring breathing mode 6a is 522 cm^{-1} (517 cm^{-1}), 6b is 687 cm^{-1} (504 cm^{-1}), and 1 is 844 cm^{-1} (829 cm^{-1}) for dimethyl-*s*-tetrazine in *p*-xylene; and for phenyl-*s*-tetrazine in benzophenone the vibrational frequency of the ring breathing 6a is 328 cm^{-1} (325 cm^{-1}), 6b is 660 cm^{-1} (656 cm^{-1}), and 1 is 796 cm^{-1} (767 cm^{-1}). The vibrational intervals observed in the neat crystal spectra were comparable with the mixed crystal intervals. The radiative lifetime of the S_1 state was calculated from absorption data (in solution at 300 K) to be $(4.5 \pm 0.2) \times 10^{-7}$ s for dimethyl-s-tetrazine and $(4.8 \pm 0.2) \times 10^{-7}$ s for phenyl-*s*-tetrazine. The fluorescence lifetime of phenyl-*s*-tetrazine in benzene (300 K) is $(14.3 \pm 1.3) \times 10^{-9}$ s, corresponding to a fluorescence quantum yield of 0.03. Weak phosphorescence signals were detected from both dimethyl-*s*-tetrazine and phenyl-*s*-tetrazine following $S_1 \leftarrow S_0$ excitation at 1.6 K. The phosphorescence lifetime of the neat crystal at 1.6 K following direct triplet photoexcitation is $(85.2 \pm 3.4) \times 10^{-6}$ s for dimethyl-*s*-tetrazine and $(59.6 \pm 1.3) \times 10^{-6}$ s for phenyl-*s*-tetrazine corresponding to phosphorescence quantum yields of ca. 10^{-3}. The major depopulating mechanism of both the S_1 and T_1 excited states is predissociation. The reaction mechanism shows a marked spin selectivity [$k(S_1)/k(T_1) = 1.4 \times 10^4$ (dimethyl-*s*-tetrazine); 4.2×10^3 (phenyl-*s*-tetrazine)] and proceeds even in dilute mixed crystals at 1.6 K to produce directly the stable products $N_2 + 2CH_3CN$ from dimethyl-*s*-tetrazine and N_2 + HCN + PhCN from phenyl-*s*-tetrazine without involving any intermediate species that was stable for an appreciable period of time.

I. Introduction

Recently some unique photochemical properties of *s*-tetrazine have been reported.[1-3] *s*-Tetrazine has consistently shown an apparent lack of intersystem crossing ($S_1 \sim\sim> T_1$) in the gas phase, in the condensed phase, and even in the low-temperature crystal. Although considerable speculation[4-6] has been given to the reported low quantum yields for fluorescence, phosphorescence, and triplet production, *s*-tetrazine has been shown to undergo photoinduced decomposition with near unit quantum yield in both gas[7] and condensed phase[1,2,8] to form the stable products N_2 and HCN.

To explore further the spectroscopy and photophysics of this interesting photochemical process dimethyl-*s*-tetrazine and phenyl-*s*-tetrazine were prepared. We report here the results of these studies. In particular, substitutional effects on the spectroscopy and the photophysical and photochemical behavior of the tetrazine chromophore have been studied at low temperatures.

Chowdhury and Goodman[9] reported the singlet–singlet absorption and emission of dimethyl-*s*-tetrazine at 300 K in the crystal and at 77 K in 3-methylpentane. The spectral origin was located at ca. 17150 cm^{-1} for both media. Hochstrasser and Marzzacco[10] identified the lowest triplet state of dimethyl-*s*-tetrazine at 13 113 cm^{-1} in absorption at 4.2 K in the crystal. They reported two vibrational intervals in the singlet–triplet spectrum. By comparison with the spectra of *s*-tetrazine and *p*-xylene they interpreted these intervals to correspond to the totally symmetric ring modes 6a′ (521 cm^{-1}) and 1′ (849 cm^{-1}). They also reported observing the 4.2 K crystal fluorescence (origin at ca. 17 100 cm^{-1}; 6a″ = 523 cm^{-1}; 1″ = 848 cm^{-1}), but were unable to detect any phosphorescence. de Vries and Wiersma[11] have recently reported the singlet–singlet absorption and fluorescence of dimethyl-*s*-tetrazine in durene at 2 K. They identified the spectral origin at 5875 Å and confirmed the upper state to be $^1B_{3u}$ ($n\pi^*$) by polarization measurements. Meyling, van der Werf, and Wiersma[8] reported the S_1 photochemical decomposition quantum yield to be 1.3 ± 0.3 and the fluorescence lifetime to be 6.0 ± 0.3 ns in the gas phase. In earlier work Strickler and Berg are reported to have determined the fluorescence lifetime[9] of dimethyl-*s*-tetrazine as 9.3 ns at 77 K and 4.1 ns at 300 K. Finally, there have been no spectroscopic or photochemical studies reported of phenyl-*s*-tetrazine.

II. Experimental Methods

2.1. Materials and Sample Preparation. Dimethyl-*s*-tetrazine was prepared by the method of W. Skorianetz and E. sz. Kováts[12] from the reaction of acetaldehyde and hydrazine [mp 67.5–68.5 °C (lit.

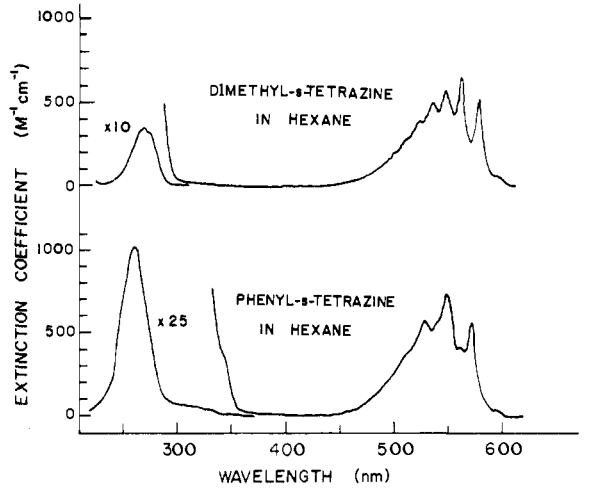

Figure 1. Absorption spectra of dimethyl-*s*-tetrazine and phenyl-*s*-tetrazine in hexane (300 K). The spectra were recorded with a Cary 14 spectrophotometer in 1-cm cells.

mp 71 °C)]. Phenyl-*s*-tetrazine was prepared by the method of O. Meresz and P. A. Foster-Verner[13] from the reaction of methyl iminobenzoate hydrochloride and hydrazine hydrate[14] [mp 125°C (lit. mp[15] 125-126 °C)]. Both the dimethyl-*s*-tetrazine and phenyl-*s*-tetrazine were purified by vacuum sublimation prior to crystal growth and film deposition.

The *p*-xylene used in our mixed crystal work was separated from a mixture of xylenes by fractional distillation. The *p*-xylene was then chromatographed in an aluminum oxide column. The host benzophenone was chromatographed into a zone melting tube and treated to 40 passes through an upright zone melter with 20 heating zones. Only the top fraction was utilized. The mixed crystals were doped at ca. 10^{-2} to 10^{-5} mol fraction and grown in the standard Bridgeman[16] manner into a low temperature bath. Good single crystals were obtained using normal crystal growth rates.

2.2. Spectroscopic Technique. Absorption spectra were recorded on a 3-m Eagle mount Baird-Atomic spectrograph. A 450-W Xe arc provided the background continuum and a 20-mA Fe-Ne hollow cathode lamp provided sharp lines for calibration purposes. Instrument slit widths of 25 μm gave spectral resolution of ca. 0.8 cm^{-1}. Kodak spectroscopic plates were used (i.e., type 103-a-F emulsion) with exposure times of typically 0.5-5 min.

Selective and pulsed excitations were achieved using a tunable dye laser optically pumped by a 100-kW Avco N_2 super radiator. The dye laser cavity contained a partially reflecting mirror, a flowing dye cell with 6° windows, a 20× beam expanding telescope, and a Czerny-Turner mounted Bausch and Lomb echelle grating with 316 grooves/mm and a 63°26′ blaze angle. Various laser dyes and mixtures of dyes were used for the active medium to give lasing in the region 4500-7000 Å.

Fluorescence and phosphorescence spectra were detected with a cooled Ga-As photomultiplier having nearly linear response from 4000 to 8500 Å. The emission was detected either broad band through suitable colored glass filters, chosen to discriminate emission from stray laser scatter, or with selectivity through a scanning monochromator with variable slits and a dispersion of 5 Å/mm. Maximum instrument resolution was ca. 0.8 cm^{-1}.

Phosphorescence lifetimes were measured following direct photoexcitation of the triplet manifold using the dye laser. The phosphorescence signal was fed directly from the cooled Ga-As photomultiplier into a 50-Ω terminated Northern Scientific signal averager. The decay was collected at 10 μs per channel (1026 channels) at a dye laser repetition rate of 50 Hz. Approximately 50 000 transient signals were averaged and fitted to a least-squares decay. The fluorescence lifetime of phenyl-*s*-tetrazine was measured using single 8-ps second harmonic pulses from an amplified, mode locked Nd^{3+} glass laser system. Samples with an *A* of 2.0 at the laser frequency (530 nm) were used. The fluorescence was filtered through an American Optical Nd 2F laser goggle (*A* of 8.3 at 530 nm) and focused on the photocathode of a fast photomultiplier (S-20). The transient was displayed on an oscilloscope (T7904) and the cathode ray tube display photographed. Fall times for the system of 1.8 ns were measured with 530-nm scatter.

III. Results and Discussion

3.1. Natural Radiative Lifetimes. The solution spectroscopy of dimethyl-*s*-tetrazine and phenyl-*s*-tetrazine were investigated. Three distinct electronic transitions were identified. The two lower energy transitions at ca. 550 and 350 nm in each species exhibited the moderate oscillator strengths and spectroscopic blue shifts in hydroxylic media characteristic of symmetry allowed singlet $\pi^* \leftarrow$ n transitions. The lowest energy singlet state of each substituted tetrazine was observed to fluoresce; the fluorescence from each species overlapped the $S_1 \leftarrow S_0$ absorption spectrum in the region of the electronic origin (ca. 570 nm). The third, higher energy transition was stronger with ϵ (270 nm) = 3450 M^{-1} cm^{-1} for dimethyl-*s*-tetrazine and ϵ (260 nm) = 25 400 M^{-1} cm^{-1} for phenyl-*s*-tetrazine, exhibited slight red shifts in hydroxylic media, and peaked in the region of the benzene $^1B_{2u}(\pi\pi^*)$ state, indicating the assignment of these transitions to benzene-like $\pi\pi^*$ states. The absorption spectra of dimethyl-*s*-tetrazine and phenyl-*s*-tetrazine in hexane at 300 K are shown in Figure 1.

The electronic origin of the $S_1 \leftarrow S_0$ transition of dimethyl-*s*-tetrazine in benzene was determined to be ca. 572 nm from the spectral overlap of absorption and fluorescence in this region. Two vibrational intervals were identified: 540 (A′) and 870 cm^{-1} (C′). The two strong absorption bands at 555 (A_0^1) and 544 nm (C_0^1) both had molar extinction coefficients of 525. The solution fluorescence peaked at 582 nm (A_1^0). Since the absorption and fluorescence spectra were qualitatively similar we were able to employ the formalism of Strickler and Berg to calculate the intrinsic radiative lifetime[17] of the dimethyl-*s*-tetrazine S_1 state to be $\tau_0 = (4.5 \pm 0.2) \times 10^{-7}$ s.

The S_1 absorption spectrum of phenyl-*s*-tetrazine at 300 K was characteristically similar to that of *s*-tetrazine and dimethyl-*s*-tetrazine. Vibrational intervals of 333 (A′) and 840 cm^{-1} (C′) were distinguished and labeled to correspond to the vibrational modes of dimethyl-*s*-tetrazine. The absorption intensity peaked at 544.5 nm (A_0^2) with a molar extinction coefficient of 602. The first strong bands in absorption and emission overlapped near 565 nm, establishing this as the electronic origin. The fluorescence peaked at 600 nm (A_2^0). The radiative lifetime of the phenyl-*s*-tetrazine S_1 state was calculated[17] to be $(4.8 \pm 0.2) \times 10^{-7}$ s. This value and the value calculated for dimethyl-*s*-tetrazine may be compared to the radiative lifetime of $(4.0 \pm 0.2) \times 10^{-7}$ s calculated for the *s*-tetrazine $^1B_{3u}(n\pi^*)$ state in benzene at 300 K.[2]

3.2. Mixed Crystal Spectroscopy. The spectral similarities in the solution spectra of *s*-tetrazine and the substituted tetrazines indicate that the lowest energy singlet-singlet transition of each of these species corresponds to the $^1B_{3u} \leftarrow {}^1A_g$ ($n\pi^*$) out-of-plane polarized electronic transition of *s*-tetrazine (D_{2h} molecular symmetry). In brief,[18] the bulk of the *s*-tetrazine spectral intensity has been shown to be contained in progressions of a single normal mode, 6a. The average vibrational frequency for this mode in the neat and mixed crystal absorption spectra was $\overline{6a'} = 704$ cm^{-1}. Another vibration was observed to have an average frequency $\overline{1'} = 1104$ cm^{-1}. A few weaker modes were identified, some apparently serving as Herzberg-Teller origins for series of the form $6a_0^n$. The spectroscopy of the substituted tetrazines is considerably more complex than that of *s*-tetrazine; however, it will be instructive to initiate our analyses by making repeated comparisons to the better understood spectroscopy of *s*-tetrazine.

We have succeeded in preparing good single crystals of dimethyl-*s*-tetrazine in *p*-xylene and of phenyl-*s*-tetrazine in benzophenone.[19] The lowest energy singlet-singlet absorption spectrum in each mixed crystal system was photographed at

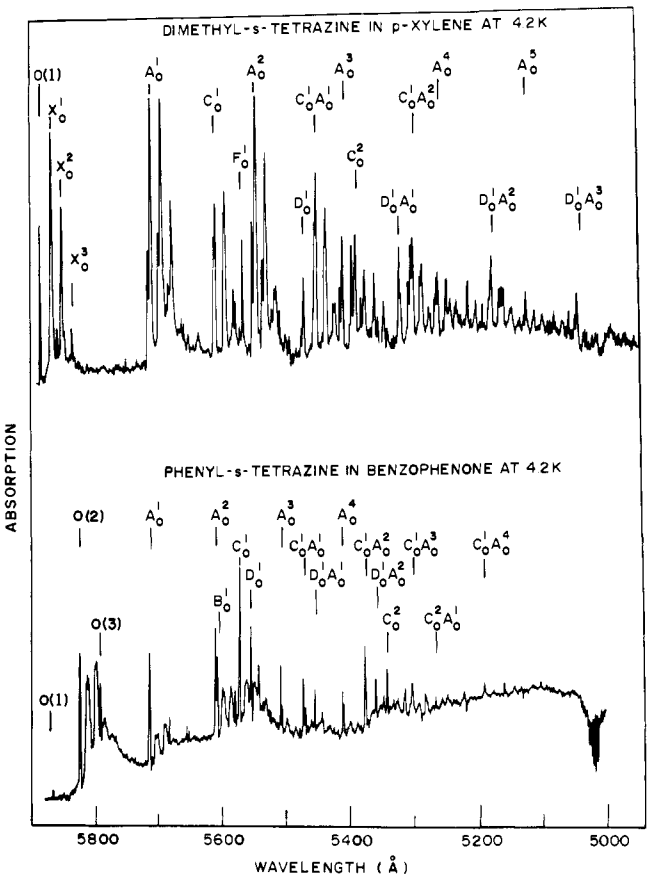

Figure 2. Singlet–singlet absorption spectra of dimethyl-*s*-tetrazine in *p*-xylene and phenyl-*s*-tetrazine in benzophenone mixed crystals at 4.2 K. The spectra were recorded photographically against a Xe continuum at 1-cm^{-1} resolution. The indices refer to various sites observed in the mixed crystal spectra.

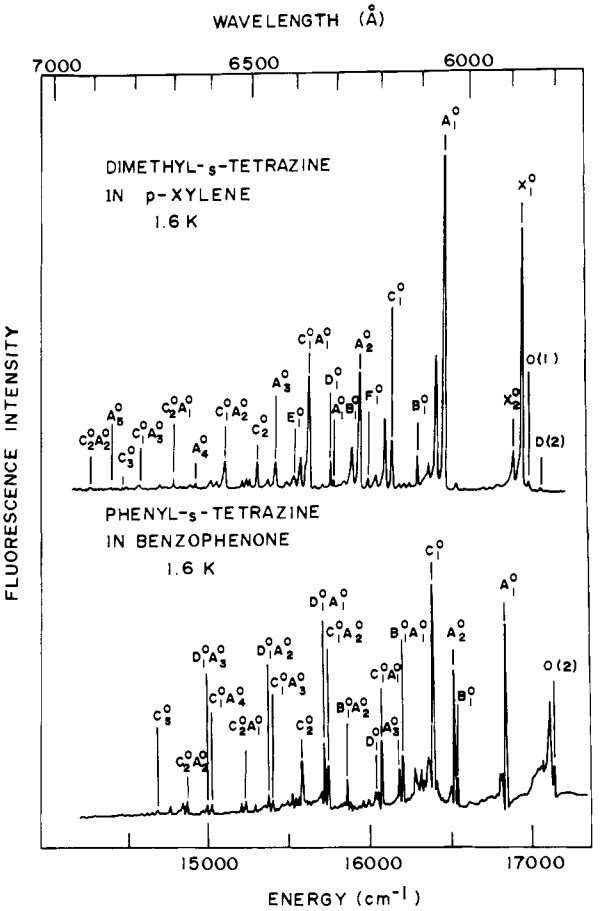

Figure 3. Laser-induced single site fluorescence spectra of dimethyl-*s*-tetrazine in *p*-xylene and phenyl-*s*-tetrazine in benzophenone following single site excitations at 1.6 K. Dye laser excitation wavelengths were 5709 Å (A_0^1 (1)) for the dimethyl-*s*-tetrazine mixed crystal and 5611 Å (A_0^2 (2)) for the phenyl-*s*-tetrazine mixed crystal. In both cases the zero phonon origin band has been reabsorbed.

4.2 K at moderate resolution; the observed spectra exhibited uniformly sharp line widths instrumentally limited at ca. 1 cm^{-1}. Direct photoexcitation of the lowest singlet state in these mixed crystals at 1.6 K resulted in moderate intensity fluorescences. The fluorescence spectra were recorded photoelectrically at 2-cm^{-1} resolution. The absorption spectra of these two mixed crystal systems are presented in Figure 2; the spectral data for absorption and fluorescence is included in Tables I and II.

Several distinct sites were identified in the low-temperature mixed crystal spectra of dimethyl-*s*-tetrazine in *p*-xylene and of phenyl-*s*-tetrazine in benzophenone. Spectroscopic evidence for the presence of sites is due to the sensitivity of electronic transition energy to chromophore environment. Each spectroscopic site arises from a different chromophore within the inhomogeneous host crystal. Following nonselective excitation both species exhibited multiple site structure in fluorescence. Single site fluorescence spectra were obtained by selective excitation with a narrow band tunable dye laser. Site selective laser-induced fluorescence spectra of dimethyl-*s*-tetrazine in *p*-xylene and phenyl-*s*-tetrazine in benzophenone at 1.6 K are shown in Figure 3; the spectral data are presented in Table II.

The mixed crystal spectra of single crystal samples of dimethyl-*s*-tetrazine in *p*-xylene at 4.2–1.6 K indicated that some 95% of the dimethyl-*s*-tetrazine chromophores were preferentially oriented in a single distinct site within the host lattice. The absorption and fluorescence origins of the dimethyl-*s*-tetrazine molecules in this particular site, site (1), coincided at 17 001 cm^{-1}. The origin appeared as a doublet in absorption with a 2.6-cm^{-1} splitting; the fluorescence origin was strongly reabsorbed.

Bands were observed in absorption at 49, 96, and 147 cm^{-1} above the origin and all the main vibronic bands. Although these transitions might have been due to the presence of various sites, site selective fluorescence and fluorescence excitation spectroscopy demonstrated that this was not the case. Selective excitation into each of these bands in turn gave rise to identical fluorescence spectra originating from the vibrationally relaxed zero-point level 0(1); fluorescence excitation spectra (obtained by monitoring the mixed crystal emission through a monochromator tuned to a fluorescence wavelength of a particular site of dimethyl-*s*-tetrazine in *p*-xylene and scanning a tunable dye laser through regions of molecular absorption) also exhibited the presence of these bands built upon the origin and vibronic bands. The regular interval and relative intensity profile for these transitions indicates that these bands (labeled X′) probably correspond to a nearly harmonic series of a low frequency torsional mode associated with the methyl groups. Similar progressions were observed in the 1.6 K fluorescence, with an average interval X″ = 50 cm^{-1}.

All major absorption transitions were polarized parallel to the electronic origin. Of the seven stronger vibrational intervals identified, those labeled X′ (49 cm^{-1}), A′ (517 cm^{-1}), B′ (504 cm^{-1}), and C′ (829 cm^{-1}) exhibited progressions of the form $A_0{}^n$. The weaker vibrations labeled D′ (1284 cm^{-1}) and F′ (970 cm^{-1}) and the 2260-cm^{-1} interval served as origins for progressions in A′ and C′. The dimethyl-*s*-tetrazine mixed crystal fluorescence spectrum was qualitatively very similar to its absorption spectrum (cf. Figures 2 and 3). Vibrational intervals of 50 (X″), 522 (A″), 687 (B″), 844 (C″), 1230 (D″),

Table I. Singlet Spectra in Mixed Crystals at 4.2 K

Dimethyl-*s*-tetrazine in *p*-xylene			Phenyl-*s*-tetrazine in benzophenone		
Line position, vac cm^{-1} (rel int)	Interval, cm^{-1}	Interpretation[a]	Line position, vac cm^{-1} (rel int)	Interval, cm^{-1}	Interpretation[b]
16 998.0 (m)	−2.6		17 098 (vw)	−69	0(1)
17 000.6 (m)	0	Origin (1)	17 167 (vs)	0	Origin (2)
17 048 (vs)	49	X_0^1	17 264 (m)	97	0(3)
17 076 (w)	77	0(2)			
17 096 (s)	96	X_0^2			
17 134 (vw)	135	0(3)			
17 146 (m)	147	X_0^3			
17 503 (m)	504	B_0^1	17 495 (s)	328	A_0^1
17 517 (vs)	517	A_0^1	17 592 (w)	425	a_0^1 (3)
17 826 (s)	826	C_0^1	17 817 (s)	650	A_0^2
17 832 (s)	832		17 824 (m)	657	B_0^1
17 969 (s)	970	F_0^1	17 914 (w)	747	a_0^2 (3)
18 007 (s)	1008	B_0^2	17 934 (vs)	767	C_0^1
18 020 (m)	1021	$B_0^1A_0^1$	17 992 (s)	825	D_0^1
18 035 (vs)	1033	A_0^2	18 031 (w)	854	c_0^1 (3)
18 272 (w)	1273		18 144 (m)	977	A_0^3
18 284 (m)	1284	D_0^1	18 152 (w)	984	$B_0^1A_0^1$
18 340 (m)	1341	$B_0^1C_0^1$	18 261 (m)	1094	$C_0^1A_0^1$
18 349 (s)	1350	$C_0^1A_0^1$	18 269 (m)	1102	E_0^1
18 474 (w)	1474	$F_0^1B_0^1$	18 319 (m)	1153	$D_0^1A_0^1$
18 486 (m)	1487	$F_0^1A_0^1$	18 355 (w)	1188	$c_0^1a_0^1$ (3)
18 523 (w)	1524	$B_0^2A_0^1$	18 466 (m)	1299	A_0^4
18 534 (m)	1535	$B_0^1A_0^2$	18 472 (w)	1306	$B_0^1A_0^2$
18 549 (w)	1550		18 480 (vw)	1313	B_0^2
18 560 (m)	1556	A_0^3	18 583 (s)	1416	$C_0^1A_0^2$
18 639 (m)	1639	C_0^2	18 641 (w)	1474	$D_0^1A_0^2$
18 755 (vw)	1756	$D_0^1B_0^1$	18 648 (vw)	1481	$D_0^1B_0^1$
18 773 (m)	1774	$D_0^1A_0^1$	18 684 (vw)	1517	$c_0^1a_0^2$ (3)
18 780 (w)	1781		18 700 (m)	1533	C_0^2
18 822 (w)	1823	$B_0^2C_0^1$	18 793 (w)	1626	A_0^5
18 835 (m)	1835	$B_0^1C_0^1A_0^1$	18 799 (w)	1632	$B_0^1A_0^3$
18 846 (m)	1847	$C_0^1A_0^2$	18 910 (w)	1743	$C_0^1A_0^1$
18 979 (m)	1979	$F_0^1B_0^1A_0^1$	— 969 (w)	1802	$D_0^1A_0^3$
18 988 (m)	1988	$F_0^1A_0^2$	19 027 (w)	1861	$C_0^2A_0^1$
19 043 (m)	2043	$B_0^1A_0^3$	19 136 (vw)	1969	B_0^3
19 059 (w)	2058		19 232 (m)	2065	$C_0^1A_0^4$
19 068 (m)	2068	A_0^4	19 350 (w)	2183	$C_0^2A_0^2$
19 170 (m)	2169	$C_0^2A_0^1$	19 467 (w)	2300	C_0^3
19 261 (m)	2260				
19 301 (w)	2301	$D_0^1A_0^2$			
19 310 (w)	2310				
19 375 (m)	2375	$B_0^1C_0^1A_0^2$			
19 387 (m)	2387	$C_0^1A_0^3$			
19 481 (w)	2481	$F_0^1A_0^3$			
19 513 (m)	2512				
19 563 (w)	2562	A_0^5			
19 646 (w)	2645				
19 774 (w)	2773				
19 823 (w)	2822	$D_0^1A_0^3$			
19 897 (w)	2896	$C_0^1A_0^4$			
19 995 (w)	2994	$F_0^1A_0^4$			
20 028 (w)	3027				
20 202 (w)	3201	$C_0^2A_0^3$			
20 338 (w)	3337	$D_0^1A_0^4$			

[a] All strong transitions exhibited progressions X_0^n with an average frequency $X' = 49\ cm^{-1}$. For convenience these transitions have not been included in this table. See Figure 2. [b] Capital letters refer to vibronic bands of the major mixed crystal site, small case letters refer to the same vibronic band built upon secondary site origins as indicated.

1451 (E″), and 994 cm^{-1} (F″) were identified and labeled to correspond with the excited state modes.

By comparing the spectroscopy of dimethyl-*s*-tetrazine, *s*-tetrazine, and *p*-xylene several vibrational intervals may be tentatively assigned. In each case two major vibrational intervals were identified. These are 517 (A′) and 829 cm^{-1} (C′) for dimethyl-*s*-tetrazine; 704 (6a′) and 1104 cm^{-1} (1′) for *s*-tetrazine; and 459 (6a′) and 829 cm^{-1} (1′) for *p*-xylene. The dimethyl-*s*-tetrazine vibrations A′ (517 cm^{-1}) and C′ (829 cm^{-1}) were determined to be totally symmetric from polarization studies. Thus the assignments of the 517- and 829-cm^{-1} intervals (522 and 844 cm^{-1} in S_1) to the totally symmetric ring breathing modes 6a and 1, respectively, seem the most secure. Based on the near degeneracy of the two normal modes 6a′ (704 cm^{-1}) and 6b′ (663 cm^{-1}) in *s*-tetrazine the two intervals of 517 (A′) and 504 cm^{-1} (B′) in dimethyl-*s*-tetrazine

Table II. Mixed Crystal Fluorescence at 1.6 K

Dimethyl-*s*-tetrazine in *p*-xylene			Phenyl-*s*-tetrazine in benzophenone		
Line position, vac cm^{-1}	Interval, cm^{-1}	Interpretation[a]	Line position, vac cm^{-1}	Interval, cm^{-1}	Interpretation[a]
17 088 ± 2	+86	0(2)	17 300 ± 2	+133	0(4)
17 037	+35	$X_1^0(2)$	17 268	+101	0(3)
17 002	0	Origin (1)	17 167	0	Origin (2)
16 952	50	$X_1^0(1)$	17 101	66	0(1)
16 905	97	$X_2^0(1)$			
16 482	520	A_1^0	16 840	327	A_1^0
16 315	687	B_1^0	16 517	660	B_1^0
16 157	845	C_1^0	16 512	665	A_2^0
16 008	994	F_1^0	16 377	800	C_1^0
15 956	1046	A_2^0	16 191	986	$B_1^0A_1^0$
15 786	1216	$B_1^0A_1^0$	16 179	998	A_3^0
15 772	1230	D_1^0	16 054	1123	$C_1^0A_1^0$
15 635	1367	$C_1^0A_1^0$	16 040	1137	D_1^0
15 551	1451	E_1^0	15 854	1323	$B_1^0A_2^0$
15 470	1532	$F_1^0A_1^0$	15 721	1456	$C_1^0A_2^0$
15 427	1575	A_3^0	15 701	1476	$D_1^0A_1^0$
15 315	1687	C_2^0	15 586	1591	C_2^0
15 247	1755	$D_1^0A_1^0$	15 397	1780	$C_1^0A_3^0$
15 112	1890	$C_1^0A_2^0$	15 364	1803	$D_1^0A_2^0$
15 026	1976	$E_1^0A_1^0$	15 263	1914	$C_2^0A_1^0$
14 927	2075	A_4^0	15 063	2114	$C_1^0A_4^0$
14 793	2209	$C_2^0A_1^0$	15 042	2135	$D_1^0A_3^0$
14 586	2416	$C_1^0A_3^0$	14 945	2232	$C_2^0A_2^0$
14 471	2531	C_3^0	14 789	2388	C_3^0
14 400	2602	A_5^0			
14 290	2712	$C_2^0A_2^0$			

[a] Spectral transitions are tabulated only for the major mixed crystal site for each chromophore. All weaker sites exhibited similar spectral features.

indicate that the dimethyl-*s*-tetrazine interval labeled B probably correlates to the normal mode 6b.

We were unable to grow useful mixed crystals of phenyl-*s*-tetrazine, in which this chromophore went substitutionally into a single well-defined lattice site. However, using benzophenone as a mixed crystal host only two strong sites were observed. These two sites, appearing with relative intensities of ca. 4:1, respectively, exhibited singlet-singlet origins 0(2) at 17 167 cm^{-1} and 0(3) at 17 264 cm^{-1}. Several weaker sites were identified (see Tables I and II) accounting collectively for about 10% of the total spectral intensity.

Absorption transitions due to phenyl-*s*-tetrazine in either site (2) or site (3) were distinguished by site selective fluorescence excitation spectroscopy. Selective excitation of either 0(2) or 0(3) resulted in distinctive yet qualitatively identical fluorescence spectra; the lines shifted by 97 cm^{-1}. The observed fluorescence originated from the vibrationally relaxed zero-point level of the photoexcited species. Four distinct optical sites were detected in the fluorescence of phenyl-*s*-tetrazine in benzophenone following nonselective excitation with an argon ion laser at 5145 Å. The four site origins were 0(1) at 17 101 cm^{-1} (vw), 0(2) at 17 167 cm^{-1} (vs), 0(3) at 17 268 cm^{-1} (s), and 0(4) at 17 300 cm^{-1} (vw).

Five vibrational intervals were identified in the 4.2 K absorption spectrum. The more intense vibrations A′ (325 cm^{-1}), B′ (656 cm^{-1}), and C′ (767 cm^{-1}) formed progressions of the type A_0^n. The weaker vibrational bands at 825 (D′) and 1102 cm^{-1} (E′) acted as vibronic origins for progressions in A′ and C′.

The 1.6 K mixed crystal fluorescence spectrum was very similar to the absorption spctrum. Vibrational intervals for the phenyl-*s*-tetrazine ground state of 328 (A″), 660 (B″), 796 (C″), and 1137 cm^{-1} (D″) were identified. By comparison with the spectra of *s*-tetrazine and dimethyl-*s*-tetrazine it seems highly probable that the two intervals 325 (328 cm^{-1} in the ground state) and 767 cm^{-1} (796 cm^{-1} in the ground state) correspond to the normal modes 6a and 1, respectively.

3.3. Neat Crystal Spectroscopy. A thin film of dimethyl-*s*-tetrazine was deposited from a 2-L bulb containing excess solid at room temperature onto a CsI optical cold finger in direct contact with liquid He. The $S_1 \leftarrow S_0$ absorption spectrum was photographed at moderate resolution with observed optical line widths of ca. 20 cm^{-1}. The neat crystal spectral data are presented in Table III. A strong origin at 17 352 cm^{-1} and vibrational intervals of 48 (X′), 514 (A′), and 820 cm^{-1} (C′) were identified. The neat crystal spectra were qualitatively and quantitatively similar to the mixed crystal spectra. Undoubtedly, better spectra could be obtained with single crystal samples, however dimethyl-*s*-tetrazine grows as needles from the vapor that are inconvenient for optical work.

The dimethyl-*s*-tetrazine fluorescence established the assignment of the singlet origin at 17 338 ± 10 cm^{-1} in the crystal. The crystal fluorescence showed several sharp lines (line widths instrument limited at ca. 3 cm^{-1}) spaced in bunches. Presumably these emissions originated from X-trap sites in the crystal. The vibronic structure was assigned in terms of four vibrational intervals: 50 (X″), 523 (A″), 843 (C″), and 1148 cm^{-1} (D″).

Weak phosphorescence was observed at 13 080 cm^{-1} following S_1 excitation at 1.6 K. The presence of phosphorescence is indicative of triplet formation via intersystem crossing from the photoexcited singlet. The integrated phosphorescence signal was approximately 10^{-4} the observed fluorescence signal.

The 4.2 K neat crystal absorption spectrum of phenyl-*s*-tetrazine was obtained for vapor grown plates of phenyl-*s*-tetrazine. The crystal line widths were ca. 10 cm^{-1}. The single crystal sample was noticeably dichroic at 300 and at 4.2 K going from red to transparent. All observed vibronic transitions appeared to be polarized ∥ to the origin (i.e., out of the mo-

Table III. Singlet Spectra in the Neat Crystal at 4.2 K

Dimethyl-*s*-tetrazine			Phenyl-*s*-tetrazine		
Line position, vac cm^{-1}	Interval, cm^{-1}	Interpretation[a]	Line position, vac cm^{-1}	Interval, cm^{-1}	Interpretation[a]
17 352 ± 10	0	Origin (1)	17 630 ± 5	−29	0(1)
17 397	45	$X_0^1(1)$	17 659	0	Origin (2)
17 447	95	0(2)	17 684	25	
			17 699	40	
			17 725	66	
			17 782	123	
			17 864	205	
17 857	505	A_0^1	17 590	291	A_0^1
17 897	547	$A_0^1X_0^1$	18 182	523	B_0^1
18 172	820	C_0^1	18 313	654	A_0^2
18 372	1020	A_0^2	18 406	747	C_0^1
18 415	1063	$A_0^2X_0^1$	18 487	827	D_0^1
18 685	1333	$C_0^1A_0^1$	18 580	921	$B_0^1A_0^1$
18 725	1373	$C_0^1A_0^1X_0^1$	18 633	974	E_0^1
18 886	1534	A_0^3	18 681	1022	A_0^3
18 936	1584	$A_0^3X_0^1$	18 740	1081	$C_0^1A_0^1$
19 004	1652	C_0^2	18 834	1175	B_0^2
19 209	1857	$C_0^1A_0^2$	18 887	1228	$D_0^1A_0^1$
19 410	2058	A_0^4	18 934	1275	$B_0^1A_0^2$
19 527	2175	$C_0^2A_0^1$	19 011	1352	$E_0^1A_0^1$
19 724	2372	$C_0^1A_0^3$	19 096	1437	$C_0^1A_0^2$
19 932	2580	A_0^5	19 141	1482	C_0^2
			19 190	1531	$B_0^2A_0^1$
			19 284	1625	$B_0^1A_0^3$
			19 350	1691	D_0^2
			19 437	1778	$C_0^1A_0^3$
			19 519	1860	$C_0^2A_0^1$

[a] Spectral transitions are included only for the major crystal site of each molecular species. All crystal sites exhibited similar vibronic structure.

Table IV. Neat Crystal Fluorescence at 1.6 K

Dimethyl-*s*-tetrazine			Phenyl-*s*-tetrazine		
Line position, vac cm^{-1} (rel int)	Interval, cm^{-1}	Interpretation[a]	Line position, vac cm^{-1} (rel int)	Interval, cm^{-1}	Interpretation[a]
17 425 (reabsorbed)	+90	0(2)	ca. 17 636 (Reabsorbed)	0	Origin
17 379 (w)	+40	X_1^0 (2)	17 603 (w)	33	
17 338 (m)	0	Origin (1)	17 592 (w)	44	Lower energy
17 293 (w)	42	X_1^0 (1)	7 5—3 (w)	53	X-trap site
			17 545 (m)	91	Origins
16 812 (vs)	526	A_1^0	17 309 (s)	327	A_1^0
16 768 (m)	570	$A_1^0X_1^0$	16 975 (vs)	661	A_2^0
16 492 (s)	846	C_1^0	16 855 (s)	781	C_1^0
16 448 (w)	890	$C_1^0X_1^0$	16 646 (m)	990	A_3^0
16 292 (m)	1046	A_2^0	16 513 (m)	1123	$C_1^0A_1^0$
16 246 (w)	1092	$A_2^0X_1^0$	16 311 (m)	1325	A_4^0

lecular plane); however, the crystal plate was too thick to obtain accurate polarization ratios. Two strong sites were identified with 0(1) at 17 630 ± 5 cm^{-1} (m) and 0(2) at 17 659 ± 5 cm^{-1} (vs). Several weaker transitions were observed to higher energy (see Table III). These bands were considerably broader and may represent either phonon modes or low frequency inter-ring torsions. Long progressions with an average vibrational interval of 361 cm^{-1} starting at the origin and the stronger vibronic bands were observed. Vibrational intervals of 361 (A′), 643 (B′), 741 (C′), 838 (D′), and 974 cm^{-1} (E′) were identified.

The 1.6 K crystal fluorescence of phenyl-*s*-tetrazine was very sharp, exhibiting zero-phonon line widths of less than a few wavenumbers. Following nonselective excitation at 5145 Å the bulk of the fluorescence intensity originated from the vibrationally relaxed zero-point levels of two particular X traps with their 0-0 bands at 17 545 (m) and 17 636 cm^{-1} (s). The fluorescence was assigned in terms of the overtone series $A_n^0(i)$ (327 cm^{-1}) and $C_n^0(i)$ (795 cm^{-1}) and progressions A_n^0 built upon $C_1^0(i)$ and $C_2^0(i)$. The indices refer to the *i*th X-trap site. Phosphorescence was detected at 13 309 cm^{-1}. The relative signal strength of the crystal phosphorescence was ca. 2×10^{-4} the fluorescence intensity. The fluorescence data for neat dimethyl-*s*-tetrazine and phenyl-*s*-tetrazine is presented in Table IV.

Although only very weak phosphorescence was observed following singlet excitation in dimethyl-*s*-tetrazine and phenyl-*s*-tetrazine at 1.6 K, stronger phosphorescence was observed in the crystal subsequent to direct triplet photoexcitation

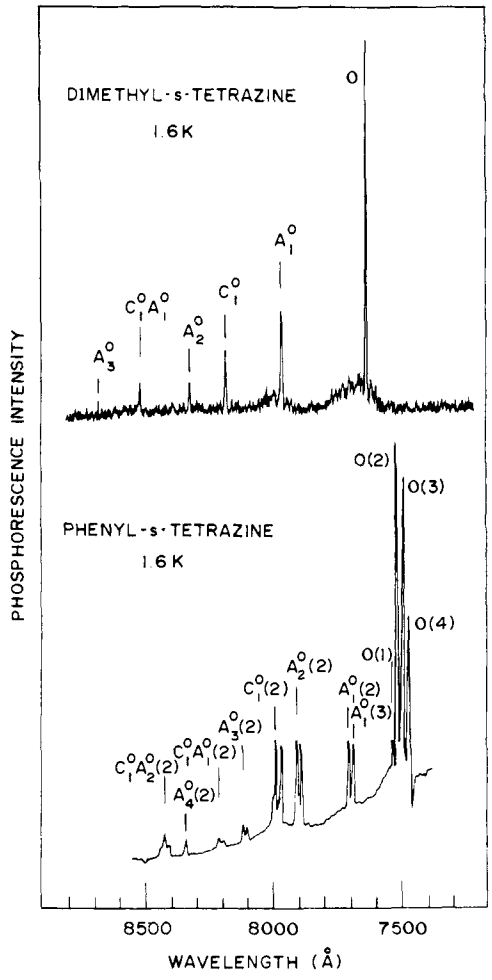

Figure 4. Neat crystal phosphorescence spectra at 1.6 K. The dimethyl-*s*-tetrazine and phenyl-*s*-tetrazine phosphorescences were detected photoelectrically with a cooled Ga/As photomultiplier tube at ca. 2-cm^{-1} resolution following laser excitation into high lying vibronic bands of the triplet manifold (i.e., 6800 Å > λ_{laser} > 6100 Å). Detector sensitivity was flat out to ca. 8400 Å, then fell off sharply.

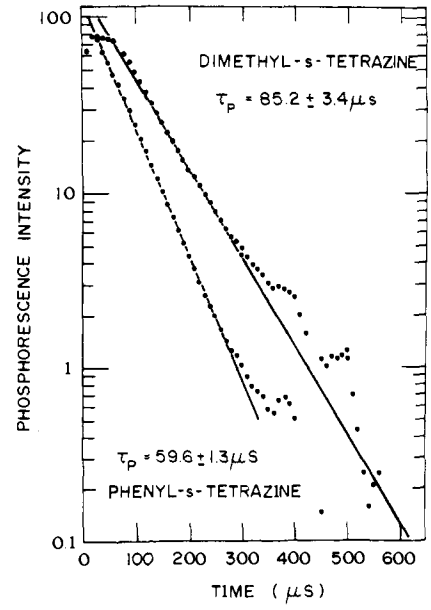

Figure 5. Phosphorescence decay of dimethyl-*s*-tetrazine and phenyl-*s*-tetrazine crystals at 1.6 K. Direct triplet state excitations were achieved with 8-ns pulses from a tunable dye laser. The resulting phosphorescence was dispersed through a monochromator and the signal characteristic of a single crystal X trap was monitored photoelectrically. Approximately 50 000 phototube transients were averaged with 10 μs temporal resolution. There was no observable variation in phosphorescence lifetime over crystal X trap.

at 6471 Å (argon ion laser). Dramatic decreases in phosphorescence intensities were observed during triplet irradiation, indicative of photoinduced decomposition of both dimethyl-*s*-tetrazine and phenyl-*s*-tetrazine.

The phosphorescence from neat dimethyl-*s*-tetrazine at 1.6 K is shown in Figure 4. The emission was characteristic of a single X-trap site with a spectral origin at 13 079 cm^{-1}. The phosphorescence was assigned in terms of the two known crystal ground state vibrational intervals: 530 (A″) and 850 cm^{-1} (C″).

Four crystal X traps were distinguished in the phenyl-*s*-tetrazine phosphorescence. Two of these, with triplet origins 0(2) at 13 302 cm^{-1} and 0(3) at 13 333 cm^{-1}, accounted for better than 99% of the observed spectral intensity. The spectra (see Figure 4) were assigned in terms of the two progressions forming ground state vibrational modes A″ (331 cm^{-1}) and C″ (793 cm^{-1}). The $C_2^0(i)$ transitions were not detected due to detector insensitivity at these wavelengths. Phosphorescence excitation spectra of neat phenyl-*s*-tetrazine determined the T_1 vibrational intervals A′ = 328 ± 5 cm^{-1} and C′ = 762 ± 5 cm^{-1}.

3.4. Excited State Photophysics. The triplet state radiative lifetime of *s*-tetrazine has been estimated[2] at 40 ms. Attempts to accurately determine the integrated absorption coefficient for the lowest triplet state (T_1) of dimethyl-*s*-tetrazine and phenyl-*s*-tetrazine were unsuccessful. In each case, saturated solutions at about 4 M exhibited peak optical densities of <0.1 in a 10-cm path in the spectral region of 6500–8000 Å. Hence triplet state lifetimes of ≳40 ms seem appropriate for both dimethyl-*s*-tetrazine and phenyl-*s*-tetrazine.

The phosphorescence lifetime of dimethyl-*s*-tetrazine and phenyl-*s*-tetrazine in the crystal at 1.6 K were measured. Direct triplet photoexcitation was achieved using 8-ns pulses from a tunable dye laser. Optimum excitation wavelengths were determined by exploring the single site phosphorescence excitation spectra of dimethyl-*s*-tetrazine and phenyl-*s*-tetrazine. The phosphorescence spectra of the major X-trap sites were known from bulk crystal excitation experiments using an argon ion laser. The crystal phosphorescence was detected photoelectrically through a monochromator tuned to the strong A_1^0 transition for dimethyl-*s*-tetrazine and the $A_2^0(i)$ transition for phenyl-*s*-tetrazine, while the dye laser was scanned through regions of the molecular triplet state absorption.

The phosphorescence decays of single X-trap sites of dimethyl-*s*-tetrazine and phenyl-*s*-tetrazine were monitored through a monochromator tuned to the strongest emission wavelength of the particular X-trap site. Characteristic decay curves for the crystal phosphorescence of dimethyl-*s*-tetrazine and phenyl-*s*-tetrazine at 1.6 K are shown in Figure 5. The decays are exponential over 4 lifetimes. The solid curves were drawn from least-squares fits giving $1/e$ excited triplet state lifetimes of τ_p = 85.2 ± 3.4 μs for dimethyl-*s*-tetrazine and τ_p = 59.6 ± 1.3 μs for phenyl-*s*-tetrazine. The corresponding value for *s*-tetrazine[18] is τ_p = 96.8 ± 2.1 μs.

Phosphorescence quantum yields for both the substituted tetrazines in the crystal at 1.6 K are in the range of 10^{-3}. The major mechanism for electronic relaxation from the photoexcited triplet state therefore must be nonradiative in nature. It is apparent (see below) that the substituted tetrazines undergo efficient photoinduced decomposition from their respective T_1 states. Since the crystal phosphorescence decays were monitored on well-defined transitions isolated by a monochromator, they represent the total decay of a particular X-trap site. The nonexponential tails observed on these decays

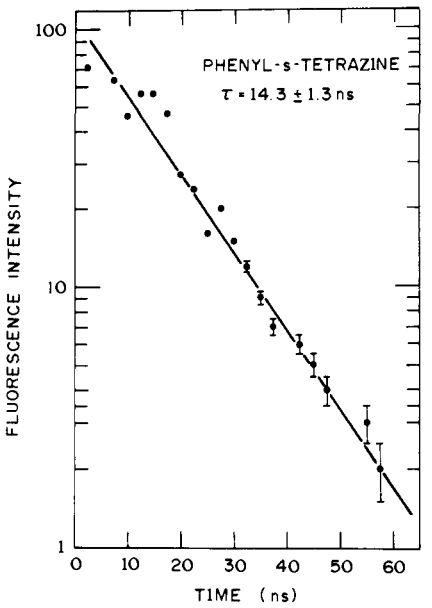

Figure 6. Fluorescence decay of phenyl-*s*-tetrazine in benzene solution. The fluorescence decay was monitored with a fast photomultiplier tube (1.8-ns fall time) following excitation via a single 530-nm pulse from a frequency doubled Nd/glass laser system. The phototube transient was displayed on an oscilloscope and photographed. The data points represent the averages (and standard deviations) of several successive experiments.

(see Figure 5) may represent the slower nonradiative decay of a second triplet spin sublevel and hence a dependence of the photochemical reaction rate on spin level. Similar results were obtained for different X traps.

The fluorescence lifetime of phenyl-*s*-tetrazine was measured in benzene solution at 300 K. Single 8-ps pulses at 5300 Å were extracted from a frequency doubled Nd^{3+} glass laser system.[20] A fall time of 1.8 ns was measured for the detection electronics with scattered 5300 Å. A plot of the fluorescence decay is presented in Figure 6. It represents a single exponential over 4 lifetimes. The solid curve is drawn from a least squares fit corresponding to a phenyl-*s*-tetrazine $1/e$ singlet state lifetime of 14.3 ± 1.3 ns, corresponding to a fluorescence yield of 3.0×10^{-2}.

3.5. Photochemical Decomposition. The substituted tetrazines are stable to thermal decomposition up to temperatures in excess of their melting points: 341 K for dimethyl-*s*-tetrazine and 398 K for phenyl-*s*-tetrazine. This is to be contrasted to the rapid thermal decomposition of *s*-tetrazine at 300 K. Dimethyl-*s*-tetrazine and phenyl-*s*-tetrazine are both photochemically active in their excited triplet or singlet states even in mixed crystals at 1.6 K. Indeed it is trivial to demonstrate the disappearance of these highly colored species in the neat or mixed crystal at 1.6 K, in solution at 300 K, and in the vapor, since upon a few minutes irradiation with a dye laser the original deep red color is lost (the photoproducts are all colorless). Low temperature infrared and Raman studies were used to identify the primary photoproducts of the lowest singlet and triplet photoreactions.

The infrared spectra at 4.2 K of neat and partially photolyzed films of dimethyl-*s*-tetrazine and phenyl-*s*-tetrazine were observed on a Perkin-Elmer 225 infrared spectrophotometer using CsI Dewar windows. The spectra were sharp, exhibiting instrument-limited line widths of a few wavenumbers. The infrared transitions of dimethyl-*s*-tetrazine and phenyl-*s*-tetrazine are listed in Table V. Single state photolysis was achieved with either a filtered Xe arc lamp (S_1), the argon ion laser 5145-Å line (S_1), or the argon ion laser 6471-Å line (T_1). The photoproducts observed following selective singlet and triplet state irradiations were identical.

Table V. Low Temperature Infrared Spectra

Dimethyl-*s*-tetrazine		Phenyl-*s*-tetrazine	
E/hc, cm^{-1}	Rel intensity	*E/hc*, cm^{-1}	Rel intensity
216 ± 2	w	398 ± 2	m
232	s	439	w
258	m	570	s
303	w	689	vs
314	m	763	s
469	vs	789	w
752	s	814	w
874	s	901	s
1009	s	916	s
1020	w	928	w
1032	vs	938	w
1091	s	1010	vw
1293	s	1031	w
1350	s	1072	m
1399	w	1102	w
1409	vs	1142	s
1432	w	1152	m
1439	s	1181	w
		1309	w
		1349	vs
		1366	w
		1382	w
		1440	vs
		1454	w
		1502	w
		1597	m
		2885	vw
		2925	vw
		3084	w

In the 4.2 K crystal photolysis of dimethyl-*s*-tetrazine there were noticeable increases in IR activity at 590, 1380, 1435, 2250, and 2970 cm^{-1}. These vibrational intervals may all be assigned to acetonitrile ($H_3CC{\equiv}N$). In the 4.2 K crystal photolysis of phenyl-*s*-tetrazine increases in IR activity at 820, 2092, and 3125 cm^{-1}; and at 545, 975, 1290, 1488, and 2230 cm^{-1} may be assigned to HCN and benzonitrile ($PhC{\equiv}N$), respectively. No other infrared transitions were observed. N_2 was detected in Raman scattering from partially photolyzed samples of phenyl-*s*-tetrazine and dimethyl-*s*-tetrazine and by fractional distillation methods after photolysis.

Both dimethyl-*s*-tetrazine and phenyl-*s*-tetrazine undergo photoinduced reactions in dilute mixed crystals and inert gas matrices at 4.2 K. In such situations there can be no chromophore-chromophore interaction, hence we conclude the decomposition to be a unimolecular process. In addition no radical or bicyclic intermediates that were stable for any appreciable time in the matrix or crystal at 4.2 K were observed following photolysis of either species. There is evidence in the literature detailing the stabilization of "Dewar" pyridine[21] and of cyclobutadiene[22] in the 8 K matrix photolysis of pyridine. We have observed no effects in the laser intensity dependence of the progress of the photodecompositions that indicate the occurrence of multiphoton processes, so we assume that one photon only is needed to dissociate one molecule. There was no indication from the present work regarding the efficiency of internal conversion from S_1 or T_1 to *thermally equilibrated levels* of the ground state. We have assumed that the photochemical yield is near unity (it was measured for dimethyltetrazine to be 1.3 ± 0.3[8]).

IV. Conclusions

The optical and photochemical studies indicate a high degree of similarity between the low lying $n\pi^*$ states of *s*-tetrazine,

dimethyl-*s*-tetrazine, and phenyl-*s*-tetrazine. Indeed it seems apparent that we are observing phenomena that can be attributed, in the main, to the tetrazine ring chromophore. Differences in the chemical physics of these species can be interpreted in view of minor perturbations on the central ring due to the presence of the substituent group(s). Such perturbations may arise from increased molecular size and therefore the number of vibrational normal modes, decreasing molecular symmetry, differing electronegativity of substituent groups compared to the tetrazine ring, and/or spin-orbit coupling factors.

The low temperature singlet and triplet $n\pi^*$ spectra are readily understood in terms of symmetry allowed transitions. The bulk of the spectral intensity occurs in members of progressions $6a_0^n$ with an average vibrational interval of 704 cm^{-1} in *s*-tetrazine, 517 cm^{-1} in dimethyl-*s*-tetrazine, and 325 cm^{-1} in phenyl-*s*-tetrazine; and $6a_n^0$ with intervals of 737, 522, and 328 cm^{-1}, respectively.

A schematic representation of the Franck–Condon pattern $6a_0^n$ for *s*-tetrazine, dimethyl-*s*-tetrazine, and phenyl-*s*-tetrazine in the mixed crystal at 4.2 K is presented in Figure 7. A one-dimensional harmonic oscillator interpretation of the progression is not unreasonable because of the dominance of the 6a (A) vibration in the optical spectra. This approximation may be least appropriate for phenyl-*s*-tetrazine. In a one-dimensional Franck–Condon treatment the observed envelope may be characterized by two parameters. These are the ratio of ground to excited state vibrational frequencies, $\delta = \omega''/\omega'$, and the shift, D, in equilibrium nuclear configuration along the particular normal coordinate following excitation. The values for δ determined from the mixed crystal data are 1.02, 1.00, and 1.00 for *s*-tetrazine, dimethyl-*s*-tetrazine, and phenyl-*s*-tetrazine, respectively. The best fit of the observed Franck–Condon envelopes to tabulated overlap integrals[23] (for $\delta = 1.00$ in each case) resulted in approximate values for D of 1.8, 1.6, and 1.4, respectively. (The overlap integrals were only tabulated for values of D in increments of 0.2.) The term D may be expressed as:

$$D = (\omega''/\hbar)^{1/2}(\mu)^{1/2}(q' - q'')$$

where $(\mu)^{1/2}$ is a reduced mass and $(q' - q'')$ is the increase in equilibrium internuclear separation upon photoexcitation. The ratios of $[(\omega''/\hbar)\mu]^{1/2}$ for *s*-tetrazine, dimethyl-*s*-tetrazine, and phenyl-*s*-tetrazine are 1.00, 1.02, and 1.08, respectively.

The ratios for D determined from the one-dimensional Franck–Condon treatment above are 1.00, 1.16, and 1.39, respectively. It is obvious, however, from Figure 7 that actual values of D for dimethyl-*s*-tetrazine and for phenyl-*s*-tetrazine are somewhat higher than those values chosen from the tables of available overlap integrals. A closer estimate, based on an interpolation of tabulated data, would place the observed D ratios at 1.00, 1.08, and 1.2, respectively. Given that the *s*-tetrazine ring undergoes only minimal geometry change upon photoexcitation to the lowest lying excited singlet state,[24] it seems likely that both dimethyl-*s*-tetrazine and phenyl-*s*-tetrazine also experience similar small changes in the chromophore ring geometry upon $S_1 \leftarrow S_0$ excitation.

Several vibrational intervals in the spectra of dimethyl-*s*-tetrazine and phenyl-*s*-tetrazine may be assigned through comparison with the corresponding spectra of *s*-tetrazine. As indicated above, the major progression forming mode, A′ (A″) with intervals of 517 cm^{-1} (522 cm^{-1}) in dimethyl-*s*-tetrazine and 325 cm^{-1} (328 cm^{-1}) in phenyl-*s*-tetrazine probably corresponds to the totally symmetric ring breathing mode 6a of *s*-tetrazine. In a similar comparison the intense vibronic bands assigned C′, with intervals of 829 cm^{-1} in dimethyl-*s*-tetrazine and 767 cm^{-1} in phenyl-*s*-tetrazine, probably correspond to the *s*-tetrazine ring mode 1 (1015 cm^{-1}). The vibrational interval labeled D′ of 1284 cm^{-1} in dimethyl-*s*-tetrazine and 825 cm^{-1} in phenyl-*s*-tetrazine may well correspond to the *s*-tetrazine ring mode 8a (1416 cm^{-1}). Finally, it appears likely that the 504-cm^{-1} interval observed in the dimethyl-*s*-tetrazine absorption spectra corresponds to the *s*-tetrazine ring mode 6b. In every instance there is, on substitution, a notable decrease in the frequency of these ring breathing modes. This is indicative of a weakening of the chromophore ring force constants and may, in part, reflect a delocalization of electron density originally associated with the methyl and phenyl substituents into the tetrazine ring.

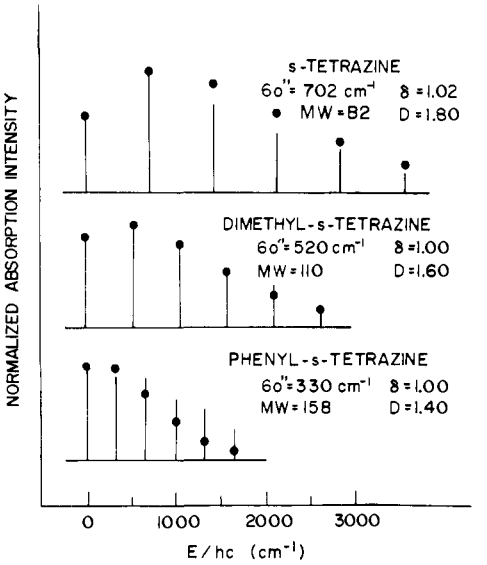

Figure 7. One-dimensional Franck–Condon envelopes for the totally symmetric ring mode 6a. Relative vibronic intensities were determined from the 4.2 K absorption spectra of *s*-tetrazine in benzene, dimethyl-*s*-tetrazine in *p*-xylene, and phenyl-*s*-tetrazine in benzophenone. The circles represent relative vibronic intensities calculated for the given parameters.

The uniform sharpness and lack of spectral congestion exhibited in the low-temperature absorption spectra and the presence of emission from the 570-nm singlet and the 760-nm triplet states of both dimethyl-*s*-tetrazine and phenyl-*s*-tetrazine indicate these states to be the lowest electronic states of each multiplicity. There was no observable line broadening either due to interference from neighboring states or a close lying continuum. All observed emission originated from the vibrationally relaxed zero-point levels of each state. No emission from unrelaxed vibronic levels was detected.

Estimates of photon utilization in the singlet and triplet state photoinduced decompositions of dimethyl-*s*-tetrazine and phenyl-*s*-tetrazine indicate the photochemical quantum yields to be very high. This is consistent with the observed rapid falloff in emission signal strengths under CW excitation and low emission quantum yields. In such a regime the total decay rates determined by the fluorescence and phosphorescence lifetime measurements will represent accurate monitors of the specific excited state photochemical reaction rate. Quantum yields of emission, intersystem crossing, and photochemistry based on this assumption for *s*-tetrazine, dimethyl-*s*-tetrazine, and phenyl-*s*-tetrazine are compared in Table VI.

Experimentally noticeable increases in relative fluorescence intensity were observed across the series *s*-tetrazine, dimethyl-*s*-tetrazine, and phenyl-*s*-tetrazine. This may be the result of decreasing photochemical activity of the substituted tetrazines. Assuming near unit quantum yields of photochemistry for all three species (i.e., no internal conversion to unreactive S_0 states) the rate of singlet state photopredisso-

Table VI. Photophysical and Photochemical Quantum Yields and Reaction Rates[a]

	s-Tetrazine	Dimethyl-s-tetrazine	Phenyl-s-tetrazine
	Singlet Excitation		
φ_F	1.1×10^{-3}	1.3×10^{-2}	3.0×10^{-2}
φ_{ISC}	$<10^{-4}$	ca. 10^{-3}	ca. 10^{-3}
$^1\varphi_{PC}$	1.00	0.99	0.97
^1k, s^{-1}	2.2×10^9	1.7×10^8	6.9×10^7
	Triplet Excitation		
φ_P	2.4×10^{-3}	2.1×10^{-3}	1.5×10^{-3}
$^3\varphi_{PC}$	0.997	0.998	0.999
^3k, s^{-1}	1.0×10^4	1.2×10^4	1.7×10^4
$^3k/^1k$	4.5×10^{-6}	7.1×10^{-5}	2.4×10^{-4}

[a] Some of the values in this table are deduced using assumptions that are discussed in the text.

ciation was decreased by a factor of 30 upon phenyl substitution.

In a related study, 1,4-*s*-tetrazine-$^{15}N_2$ was synthesized to assess the importance of 1,4-nitrogen-nitrogen bonding[3] in the tetrazine photolysis mechanism. State selective photolyses of the 1,4-*s*-tetrazine-$^{15}N_2$ were performed in the vapor and solid at 300 K. The photoproducts were fractionally distilled into a mass spectrometer. Mass analysis of the photoproducts indicated in every instance the presence of $^{14}N^{15}N$(*m/e* 29) and a 1:1 mixture of isotopic HCN (*m/e* 27 and 28). No $^{15}N_2$ (*m/e* 30) was observed, indicating 1,4-nitrogen cross ring bonding to play a negligible role in the overall decomposition mechanism. In view of the aforementioned similarities between *s*-tetrazine, dimethyl-*s*-tetrazine, and phenyl-*s*-tetrazine, and of the absence of observable intermediate species in the photochemistry of each species, we do not anticipate that such cross ring bonding occurs in the photoinduced decompositions of dimethyl-*s*-tetrazine and phenyl-*s*-tetrazine.

It is of interest to compare the relative energies of the various tetrazines and their respective photoproducts. The thermochemistry[2] of the *s*-tetrazine ground state reaction was estimated to be $\Delta H \geq -1$ kcal mol^{-1}. We do not expect the dimethyl-*s*-tetrazine or phenyl-*s*-tetrazine reactions to become highly exothermic. Thus to a first approximation the enthalpy of a given photoinduced reaction is equal to or slightly greater than the excitation energy. The observed photoproducts (HCN, CH_3CN, C_6H_5CN, and N_2) all have singlet ground states. The lowest energy singlet and triplet states of dimethyl-*s*-tetrazine and phenyl-*s*-tetrazine lie at about 17 500 and 13 300 cm^{-1}, respectively. The corresponding *s*-tetrazine states are found to slightly higher energies. The first electronically excited state of each of the various photoproducts is a triplet state. This lowest triplet is located at ca. 50 200 cm^{-1} in N_2, 50 000 cm^{-1} in HCN, 35 000 cm^{-1} in acetonitrile, and 20 000 cm^{-1} in benzonitrile (the lowest energy excited singlet state is several thousands of centimeters^{-1} higher in energy in each case). There is, therefore, inufficient energy to produce electronically excited photoproducts and we should expect to observe the generation of product species whose only excitation involves vibrational and rotational levels of the ground electronic states.

Small, but significant substitutional effects were observed in the phosphorescence lifetime measurements of dimethyl-*s*-tetrazine and phenyl-*s*-tetrazine. The singlet and triplet state predissociations apparently both yield ground state primary photoproducts (i.e., singlets). The observed triplet state decomposition is therefore a spin-forbidden process. This is to say that the triplet reaction proceeds through the admixture of singlet character into the triplet state through a spin-orbit or vibronic spin-orbit coupling mechanism. The ratio of the

Scheme I

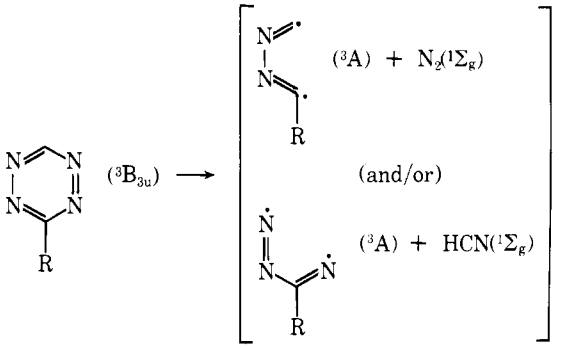

triplet photopredissociation rate, ^3k, to the singlet rate, ^1k, determines to a first approximation the degree of spin selectivity of the reaction. The ratio $^3k/^1k$ increases from 4.5×10^{-6} for *s*-tetrazine to 2.4×10^{-4} for phenyl-*s*-tetrazine, indicative of almost a 50-fold decrease in spin selectivity of this reaction mechanism upon phenyl substitution. On the other hand it is conceivable that the triplet reaction proceeds through the triplet state of an intermediate of the type shown in Scheme I. Experiments are in progress here to explore these pathways.

Status of Photodissociation Mechanism. The available experimental data on excited state structures, effects of substituents, and nonradiative lifetimes provide information regarding the nature of the photodissociation of *s*-tetrazine. It would be useful to know whether the dissociation into HCN and N_2 can be rationalized from the electronic and nuclear coordinate changes that occur on excitation. A recent calculation of the wave functions and energies of the states of *s*-tetrazine at the ground state nuclear configuration[6] indicate that the $(A)^{1,3}B_{3u}$ states are described predominantly by an electron promoted from the b_{3g} nonbonding (approximate description) orbital into the $a_u(\pi^*)$ orbital. This results in a state whose wave function is both n and π antibonding across the N-N bonds. This state cannot therefore correlate smoothly with ground state N_2. The Franck-Condon patterns of the substituted tetrazine spectra indicate that the molecular geometry changes on excitation are similar in each case, that they are very slight, and that they are essentially the same changes as occur on the excitation of *s*-tetrazine. On the other hand the rate of the photodissociation varies markedly amongst this group of compounds, as evidenced by the changes in fluorescence decay times. Therefore, there is no reason to suppose that the geometry changes that occur on excitation (i.e., a change in 6a) are signaling the pathway of the photodissociation. Neither does the change in electronic structure, viewed as a simple orbital promotion, point clearly to an initial step for the reaction. The excitation of an n electron (which is, of course, delocalized in the σ bonds) may result in the breaking of one N-N bond, since there exists some probability that the resulting π antibonding electron will fully antibond a particular pair of N atoms that are simultaneously bound by only one σ electron. This electronic rearrangement would result in dissociation into a biradical form that may then produce HCN and N_2 as observed. The activation needed for this path is just the breaking of one σ bond. However, our results do not distinguish between such a mechanism, based on elementary considerations related to the electronic distribution, and one that involves a predissociation of $^{1,3}B_{3u}$ states into high vibrational levels of the ground state.

The dissociation of the tetrazines takes ca. 500 ps or longer, but we can be certain that in the low temperature condensed phase the initially formed (by internal conversion) ground-state distribution could not persist for times much longer than ca. 1 ps. We know that vibrational relaxation occurs much more

rapidly than the photochemical reaction, because we have found the fluorescence yield to be wavelength insensitive in the region of the S_1 absorption even for large energy excesses. We therefore can conclude that the rate controlling step in such a predissociation is the transition from the bound $^1B_{3u}$ states of the *s*-tetrazines to the ground state (discrete and/or continua) levels. In view of the fact that the quantum yield of the reaction is so close to unity, it is certain that these high levels of the ground state do not live long enough to be relaxed to unreactive species.

Some additional insight to the considerations of the previous paragraph is gained from a knowledge of the densities of ground state levels at the energies of the S_1 and T_1 states. From the Haarhoff formula[25] we obtain 1.1×10^6 and 1.6×10^7 cm for the total numbers of states per wavenumber (ζ) at the excess energies corresponding to the 0-0 bands of the T_1 and S_1 states, respectively. Thus, ζ_S/ζ_T is 15. It should be recalled that the photodissociation from T_1 is ca. five orders of magnitude slower than that from S_1. In view of our spectral analysis we are able to obtain harmonic oscillator Franck-Condon factors for three of the four totally symmetric modes. Unfortunately the 3000-cm^{-1} C-H stretch is not observed in our spectra, so we have assumed it to have a $0 \rightarrow 1$ Franck-Condon factor that is two orders of magnitude less than 6a. On the basis of this assumption the largest terms by far in the coupling of both S_1 and T_1 to the ground state involve those high-frequency modes in association with small (1-5) numbers of quanta of 6a, and one or other of the b_{3u} modes to provide the proper symmetry for the final states. The Franck-Condon factors we have calculated are comparable (they do not differ by more than a factor of 10) for the S_1 and T_1 excess energies. The point of these estimates is to demonstrate that the large difference in the reaction rate observed via the light emission from singlet and triplet states is not caused only by differences in the coupling and density of states terms such as would appear in a statistical model (Fermi's golden rule) for the predissociation into the ground state. This result is important, since it suggests that states of biradical intermediates are unlikely to be directly coupled to S_1 or T_1 of tetrazine. Biradicals are expected to have both singlet and triplet states that are nearby in energy and so there might be no spin prohibition on the predissociation to essentially biradical type states. On the other hand if the ground state levels of bound *s*-tetrazine were essential for the predissociation, i.e., as an intermediate in the photodissociation, then the predissociation of S_1 would be expected to occur ca. 10^5 times faster than T_1 because of spin selection rules, which is the observation.

In the event that the highly excited ground state levels are involved in the reaction, and that the couplings of these levels to S_1 and T_1 are the rate determining steps, the relationship between the reaction pathway and the observed spectroscopic properties of these bound states is expected to be subtle. For example the calculations of Franck-Condon factors and effective densities of states based on measured values of the needed parameters yields the result that the most strongly interacting states involve C-H stretches that are not even observed in the spectra. Thus, although the excited state geometry is only infinitesimally shifted along the C-H coordinate from the ground state value, most of the highly excited ground state levels reached by predissociation probably involve this mode and 6a in association with an out-of-plane mode.

Acknowledgment. This research was supported by a grant from the National Science Foundation (to R.M.H. and A.B.S.) and by the National Science Foundation MRL program at The University of Pennsylvania (No. DMR 76-00678).

References and Notes

(1) R. M. Hochstrasser and D. S. King, *J. Am. Chem. Soc.*, **97**, 4760 (1975).
(2) R. M. Hochstrasser and D. S. King, *J. Am. Chem. Soc.*, **98**, 5443 (1976).
(3) D. S. King, C. T. Denny, R. M. Hochstrasser, and A. B. Smith III, *J. Am. Chem. Soc.*, **99**, 271 (1977).
(4) A. J. Merer and K. K. Innes, *Proc. R. Soc., London, Ser. A*, **302**, 271 (1968).
(5) J. R. McDonald and L. E. Brus, *J. Chem. Phys.*, **59**, 4966 (1973).
(6) T-K Ha, *Mol. Phys.*, **29**, 1829 (1975).
(7) R. R. Karl, Jr., and K. K. Innes, *Chem. Phys. Lett.*, **36**, 275 (1975).
(8) J. H. Meyling, R. P. van der Werf, and D. A. Wiersma, *Chem. Phys. Lett.*, **28**, 364 (1974).
(9) M. Chowdhury and L. Goodman, *J. Chem. Phys.*, **38**, 548 (1962); **38**, 2979 (1963).
(10) C. J. Marzzacco, Ph.D. Thesis, University of Pennsylvania, 1968.
(11) H. de Vries and D. A. Wiersma, *Phys. Rev. Lett.*, **36**, 91 (1976).
(12) W. Skorlanetz and E. sz. Kováts, *Tetrahedron Lett.*, 5067 (1966).
(13) O. Meresz and P. A. Foster-Verner, *J. Chem. Soc., Chem. Commun.*, 950 (1972).
(14) We wish to acknowledge the assistance of Mr. E. D. Plotzker in the preparation of the substituted tetrazines.
(15) V. A. Grakauskas, A. J. Tomasewski, and J. P. Horwitz, *J. Am. Chem. Soc.*, **80**, 3155 (1958).
(16) P. W. Bridgeman, *Proc. Am. Acad.*, **60**, 305 (1925); also see D. C. Stockbarger, *J. Opt. Soc. Am.*, **39**, 731 (1949). and H. Guggenheim, *J. Appl. Phys.*, **34**, 2482 (1963).
(17) S. J. Strickler and R. A. Berg, *J. Chem. Phys.*, **37**, 814 (1962).
(18) R. M. Hochstrasser and D. S. King, *Chem. Phys.*, **5**, 439 (1974).
(19) A perfect mixed crystal is one in which the guest chromophore is incorporated substitutionally at reasonable concentration into the host crystal lattice. Thus, by orienting the host crystal one knows the orientation of the guest molecules exactly. There are unfortunately no hard and fast rules for choosing an appropriate host. The choice of host species for *s*-tetrazine (pyrazine and benzene) and dimethyl-*s*-tetrazine (*p*-xylene) were straightforward. However, in our search for a good mixed crystal system for the study of phenyl-*s*-tetrazine we tried benzene, phenylpyrrole, 4-phenylpyridine, 4-phenylpyrimidine, biphenyl, dibromo diphenyl ether, and benzophenone. In every instance, except benzophenone, we observed complete rejection. Even in benzophenone the rejection rate is high (maximum solubility of ca. 10^{-5} M/M) and there is evidence of crystal strain. It appears that phenyl-*s*-tetrazine may offer the opportunity to study the dynamics of solid solubility. We are in the process of investigating several other distinctive species for phenyl-*s*-tetrazine mixed crystal hosts. The results of this work (principally due to the efforts of Dr. A. McGhie) will be published elsewhere.
(20) R. W. Anderson, Jr., and R/ M. Hochstrasser, *J. Phys. Chem.*, in press.
(21) K. E. Wilzbach and D. J. Rausch, *J. Am. Chem. Soc.*, **92**, 2178 (1970); also see M. G. Barlow, R. N. Haszeldine, and J. G. Dingwall, *J. Chem. Soc., Perkin Trans. 1*, 1542 (1973).
(22) O. L. Chapman, C. L. McIntosh, and J. Pacansky, *J. Am. Chem. Soc.*, **95**, 614 (1973).
(23) J. R. Henderson, R. A. Willett, M. Muramoto, and D. C. Richardson, "Tables of Harmonic Franck–Condon Overlap Integrals Including Displacement of Normal Coordinates", Douglas Report SM-45807 (1964).
(24) D. H. Levy, private communication (1976).
(25) P. C. Haarhoff, *Mol. Phys.*, **6**, 337 (1963).